Rock physics based probabilistic lithology and fluid prediction in a heterogeneous carbonate reservoir

Luanxiao Zhao[1,2]*, *Jianhua Geng*[1], *De-hua Han*[2], *Jiubing Cheng*[1] *and Tonglou Guo*[3]
[1]*Tongji University*, [2]*University of Houston*, [3]*Exploration Southern Branch, SINOPEC*

Summary

The deep-buried Paleozoic marine carbonate reservoirs of Sichuan Basin, SW China, exhibit strong heterogeneities due to complicated diagenetic processes. The goal of our work is to map posterior probabilities of lithology and fluid based on seismic and well observations in this reservoir, thus helping characterize reservoir complexity. Rock physics study gives physical insight on how the elastic properties of different litho-fluid classes can be distinguished. Bayesian linearized AVO inversion results indicate that the posterior distribution of P-wave and S-wave velocity are confidently extracted, while the inverted density tends to show high uncertainty due to a lack of wide angle of seismic data. Finally, a full Bayesian approach was implemented to propagate uncertainty from prestack seismic data to assess posterior probabilities of litho-fluid classes in an integrated framework.

Introduction

Probabilistic lithology/fluid prediction from prestack seismic data often entails both the uncertainty of seismic inversion to elastic properties and that of the link between lithofacies to elastic properties. It has been studied by many authors on the methodic aspect or the application aspect (e.g., Eidsvik et al., 2004; Larsen et al., 2006; Buland and Omre, 2008; Ulvmoen and Omre, 2010). However, most of those work focused on sandstone reservoir with relative less heterogeneity. It is still very challenging to demonstrate its application to deep-buried carbonate reservoirs with strong heterogeneities as studied in this paper. First of all, the deep target reservoir makes it hard to obtain wide angle gather, making the seismic inversion difficult to extract elastic parameters reliably. Secondly, the complex diagenesis complicate rock physics relationship in carbonate, which in turn make seismic response poorly understood. Understanding the sensitivity of elastic properties of carbonates responding to fluids in heterogeneous reservoir rocks is critical to test the feasibility of lithology and fluid prediction from seismic attributes.

In this paper, we focus on demonstrating how the geological understanding and rock physics can help us better constrain the lithofacies prediction from seismic data in a probabilistic framework. The studied carbonate reservoirs represent evaporitic carbonate platform edge depositional environment, and the diagenesis process is very complex and thereby strongly reorganize the pore space. The main diagenetic processes include compaction-pressure solution, selective dissolution, fracturing, dolomitization, and recrystallization. The target inversion zone defines in-lines 209 and cross-lines from 100-250. Stacked image of the target zone is shown in Figure 1, on which a red vertical line indicates the location of the available well.

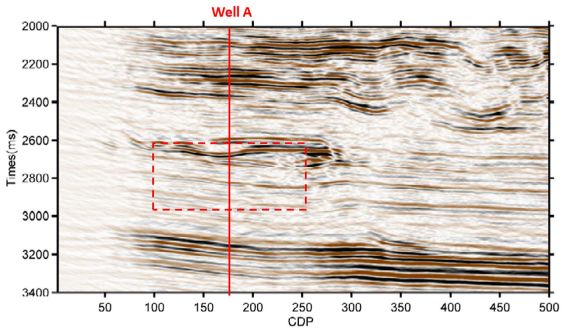

Figure 1: Stacked seismic image of in-line 209. The dashed rectangle in Figure 5a identifies the target volume, and the red lines identify the well A.

Rock physics analysis

Well observations (P-wave velocity, S-wave velocity and density) are displayed as a function of two-way travel time in Figure 2. Based on the well observations as well as geological knowledge, we define four lithofacies classes in the target inversion zone: anhydrite, dolostone, gas-carbonates and limestone. Gas-carbonates are found from the depth of 2680ms to 2730ms between two intervals of brine-saturated dolostone. Geological observations suggest that the pore space in reservoir rocks is dominated by secondary porosity. Figure 3 shows core plugs representative of the carbonate reservoir formation in Sichuan Basin. It is evident to see that the heterogeneous pore systems are related to small-scale touching vugs (grain molds) and micro-fractures. Typically, most of the fluid storage is in the vuggy system and most of the flow capacity is in cracks.

We use effective-medium modeling to examine how vuggy-fracture porosity system and fluid behavior together may affect the elastic properties. The dry-rock elastic moduli were computed using the differentiated effective

DOI http://dx.doi.org/10.1190/segam2013-0486.1

medium theory (Mavko et al., 2009). In this case, the pore space was assumed to consist of a combination of stiff matrix porosity (vuggy pores) and micro-fractures with aspect ratio 0.4 and 0.01 respectively. The matrix porosity is assumed as 0.05, the crack density ranges from 0 to 0.30. The mineralogy was taken to be dolomite. The moduli of the saturated rock at low frequencies were computed based on the dry moduli and Gassmann's equations.

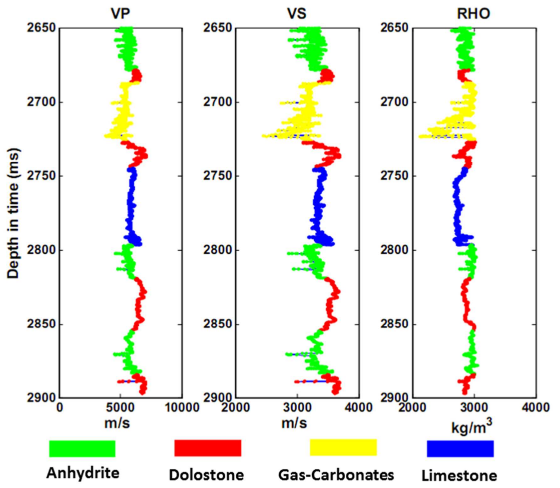

Figure 2: P-wave velocity, S-wave velocity and density are displayed as a function of two-way travel time in well A. Litho-fluid classes are defined here.

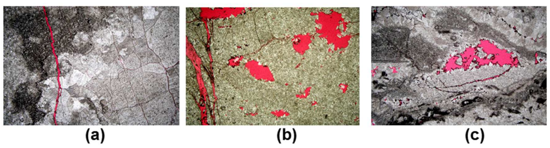

Figure 3: Core photos of reservoir rocks in studied field of Sichuan Basin, SW china. Red parts represent pore space.

Simulated elastic properties of the carbonate's Vp/Vs ratio versus P-impedance are displayed in Figure 4. Two back lines indicate 100% gas saturated and 100% brine saturated, the dashed pink lines represent modeling result with different crack density. All of the scattering data points are from the log data in Well A. The rock physics model explains the scattering point in terms of fluids and porosity heterogeneities. Gas has a strong effect in reducing P-impedance and Vp/Vs ratio for fractured carbonate, and this effect is stronger with higher crack density. However, the brine saturated fractured carbonates exhibit a different elastic response. Physically, when the fractures are dry or filled with gas, the seismic propagation velocity which is normal to the fracture will be significantly decreased. In contrast, the brine drastically stiffens the very compliant fractures (Schoenberg and Sayers, 1995). The scattering dots of gas-carbonates are in good agreement with model prediction, which also indicate the reservoir rocks are heavily fractured. It is clear to see that gas-carbonate in this reservoir can well separate from other three faceis classes, and the anhydrite, dolostone and limestone can also be distinguished to certain degree.

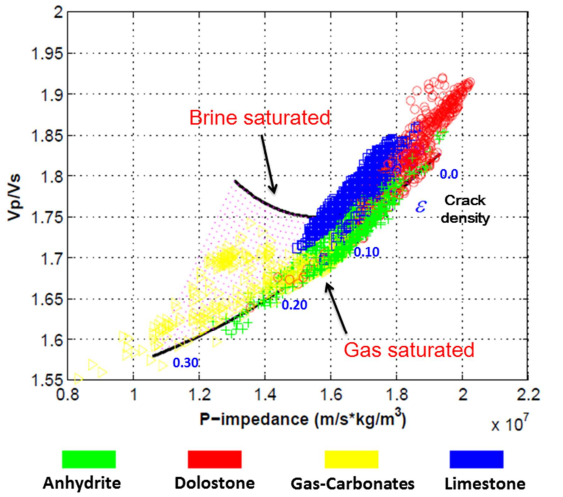

Figure 4: A rock physics template presented as cross-plots of Vp/Vs versus P-impedance which is used to illustrate the fluid sensitivity and crack density effect.

Probabilistic lithofacies inversion

In our current study, we make inferences about the defined categorical lithofacies from prestack seismic data following the fast Bayesian inversion method presented by Buland et al. (2008). The Lithology/fluid characteristic **f** and seismic data **d** can be linked via a set of elastic parameters **m**. The method propagates uncertainty from seismic data to litho-fluid classes by integrating two conditional probabilities. The first is the probability of elastic properties estimated from seismic data by using a Bayesian AVO inversion approach (Buland and Omre, 2003). The second is the probability of litho-fluid classes conditioned by elastic attributes based on statistical rock physics. In a Bayesian inversion setting, the posterior distribution for **f** given the seismic gather **d** generally can be expressed as

$$p(f|d) = \int \dots \int p(f|m)p(m|d)dm \qquad (1)$$

and the $p(f|m)$ and $p(m|d)$ can be defined as:

$$p(f|m) \propto p(m|f)p(f) \qquad (2)$$

$$p(m|d) \propto p(d|m)p(m) \qquad (3)$$

DOI http://dx.doi.org/10.1190/segam2013-0486.1

The detailed workflow for numerical calculation of the posterior probabilities for the facies classes is described and illustrated in Buland et al. (2008). It should be noted that we do not take into account prior spatial information about the lithology/fluid classes to assess the posterior model.

We simultaneously invert P- wave velocity, S-wave velocity and density following the Bayesian AVO inversion approach presented in Buland and Omre (2003). The inversion results of well position (Figure 5) show that the inverted P-wave velocity and S-wave velocity fit quite well with well log trend, and even some details of the vertical change can be captured. However, the inverted density is not accurate enough to be retrieved at the well position. The 0.9 prediction interval indicates that the uncertainty of the inverted P- or S-wave velocity is also much lower than that of the inverted density. This may be partially resulted from the realistic noise levels and lack of reflectivity data of wide angle gather in deep targeted formation. In order to decrease the uncertainty of the litho-fluid facies prediction and obtain a more reliable inversion result, we will not use density information as the input of lithology/fluid inversion.

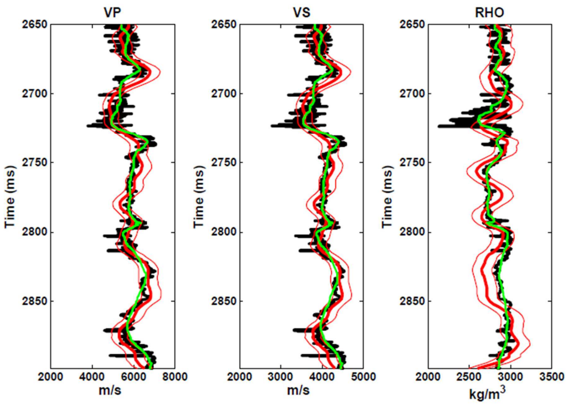

Figure 5: Inversion result of well log(black line indicates the actual well log data, green line indicates well log trend, red thick line indicates maximum a solution, red thin line indicates 0.9 prediction interval)

The rock physics likelihood $p(m|f)$will be simulated from statistical rock physics analysis of the available log data in Well A. The rock physics likelihoods displayed in Figure 6 are assumed to be Gaussian distribution, and can be calculated from the associated expectation and variances for the four lithofacies. The elastic properties of gas-carbonates can separate well with other three lithofacies, but the variance and associated uncertainty tend to be higher. While the elastic properties of the anhydrite, limestone and dolostone are overlapping with each other to some degrees, but they show relatively lower variance and associated uncertainty. The prior probabilities p(f)assigned to the each defined facies classes are 0.25.

Results of lithology and fluid prediction

Following the approach presented in the previous sections, we will show the results of probabilistic lithology and fluid inversion in the target zone. Figure 7 displays the posterior probability for anhydrite, dolostone, gas-carbonates and limestone in the well position. The sum of posterior probability of each lithoface is equal to 1, and for a perfect prediction, the probabilities would be one in the position of reference LF classes and zero otherwise. Generally speaking, the predicted posterior probabilities for lithofacies are acceptable when compared with the actual lithology profile defined in the well position. We can observe that the probabilities of gas-carbonates occurrence at the reservoir zones (2700ms-2740ms) are about 0.6-0.7, which demonstrate that the gas-carbonates are highly predictable. This is mainly due to two reasons. First of all, the seismic inversion results to the elastic properties have a good match with actual log data and the associated uncertainty is low in the gas-carbonate zone. Secondly, the elastic properties for the gas-carbonates have a good separation with other lithofacies. Errors sometimes occur for discriminating anhydrite, dolostone and limestone, this can be expected from the overlapping elastic properties based on the rock physics likelihood.

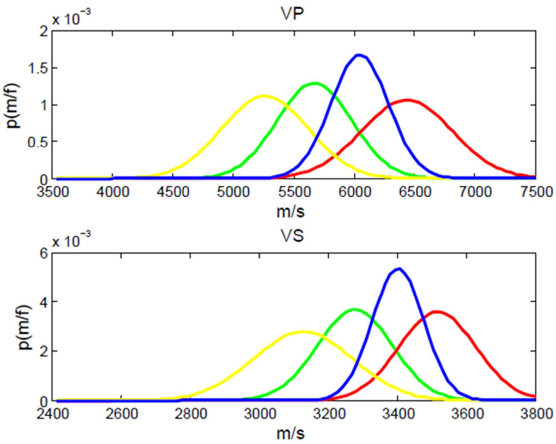

Figure 6: The rock physics likelihood functions of Vp and Vs for the four lithofacies. The yellow, green, blue and red colors represent the litho-fluid classes of gas-carbonates, anhydrite, limestone and dolostone, respectively.

The posterior probability of gas-carbonate and anhydrite, dolostone, and limestone for the inline 209 are displayed in Figure 8 and Figure 9, on which lithofacies profile from well A is also marked to compare with the prediction result. The inversion result suggests that the reservoir zones appear in the top of the target zone (2700ms-2750ms) with varying posterior probabilities from 0.5 to 0.8. Although the inversion procedure goes trace by trace, without

DOI http://dx.doi.org/10.1190/segam2013-0486.1

considering the lateral continuity, the predicted probabilities of the gas-carbonates area still show pretty geological consistence. We also map the posterior probabilities of anhydrite, dolostone and limestone. The target zone show significant heterogeneities in terms of lithology distribution, which is mainly dependent on the varying depositional environment and strong digenesis in the geological history. Even the prediction uncertainty might be very high in certain areas, it is still very useful to help us delineate the reservoir architecture and construct the geological model.

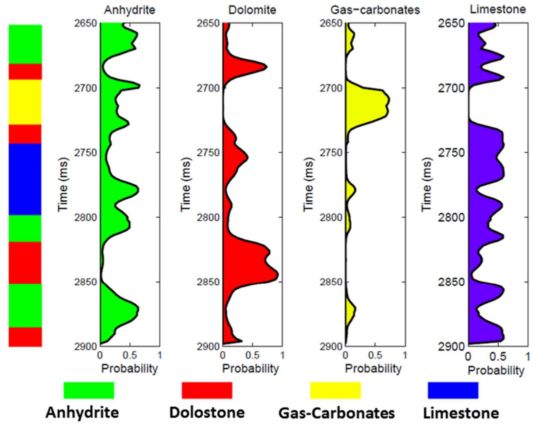

Figure 7: (Left) The reference lithology and fluid profile which is defined based on well log analysis. (Right) Posterior probabilities for lithofacies prediction from seismic data at the well position.

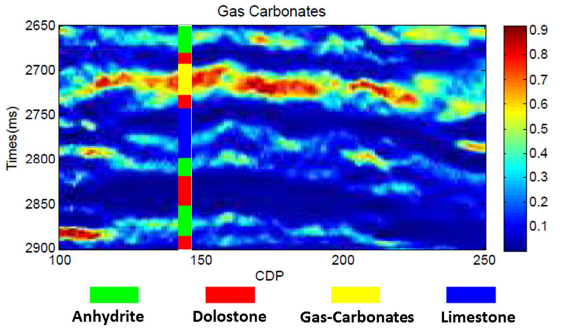

Figure 8: Posterior probability for gas-carbonates distribution in the target reservoir.

Conclusions

Lithology and fluid prediction from seismic data in Sichuan Basin, SW china is significantly challenging due to its deep burial depth and substantial pore-fabric heterogeneity. With integration of geological information, rock physics analysis, well log data and seismic data, we applied a fast Bayesian inversion approach to predict the posterior probabilities for the defined litho-fluid classes. Based on geological understanding of the reservoir, the employed rock physics modeling scheme gives us physical insight about how the litho-fluid classes with different rock properties can be related to their corresponding elastic properties, as well as the degree of separation. We concluded that the elastic response of carbonates can be sensitive to the fluid effect due to the presences of vuggy-fracture pore system in this reservoir. For the studied deep target carbonate reservoir, the density prediction is not reliable with high uncertainty due to the lack of wide angle seismic data. Therefore, we only use P-wave velocity and S-wave velocity for lithology and fluid prediction. We further map the posterior probability for the four defined litho-fluid classes in the target zone and identify the potential gas-carbonate formation with geologically spatial consistence. The case study also illustrates the prediction strength comes from both the uncertainty of rock physics likelihood and the seismic inversion results.

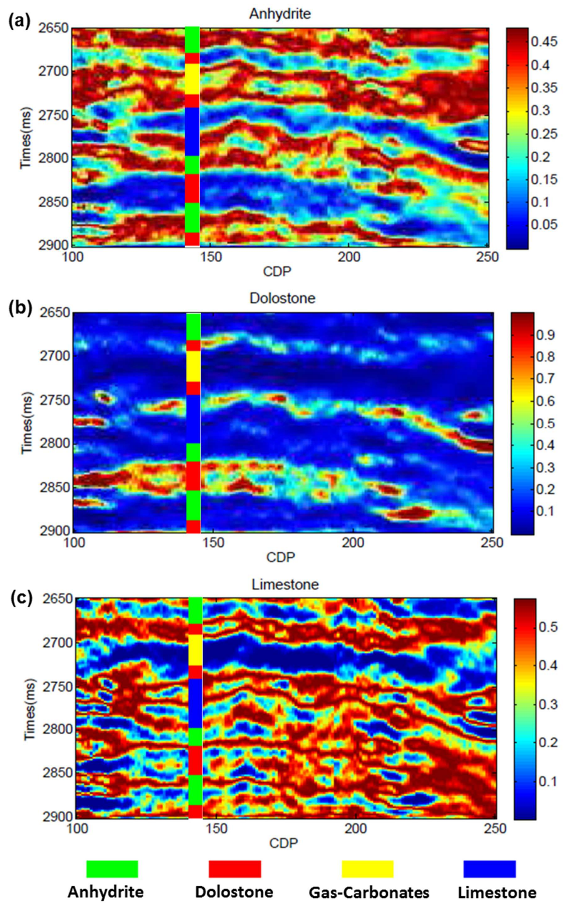

Figure 9: Posterior probabilities for anhydrite, dolostone and limestone distribution in the target reservoir.

DOI http://dx.doi.org/10.1190/segam2013-0486.1

http://dx.doi.org/10.1190/segam2013-0486.1

EDITED REFERENCES

Note: This reference list is a copy-edited version of the reference list submitted by the author. Reference lists for the 2013 SEG Technical Program Expanded Abstracts have been copy edited so that references provided with the online metadata for each paper will achieve a high degree of linking to cited sources that appear on the Web.

REFERENCES

Buland, A., and H. Omre, 2003a, Bayesian linearized AVO inversion: Geophysics, **68**, 185–198, http://dx.doi.org/10.1190/1.1543206.

Buland, A., O. Kolbjørnsen, R. Hauge, Ø. Skjæveland, and K. Duffaut, 2008, Bayesian lithology and fluid prediction from seismic prestack data: Geophysics, **73**, no. 3, C13–C21, http://dx.doi.org/10.1190/1.2842150.

Eidsvik, J., P. Avseth, H. Omre, T. Mukerji, and G. Mavko, 2004, Stochastic reservoir characterization using prestack seismic data: Geophysics, **69**, 978–993, http://dx.doi.org/10.1190/1.1778241.

Larsen, A. L., M. Ulvmoen, H. Omre, and A. Buland, 2006, Bayesian lithology/fluid prediction and simulation on the basis of a Markov-chain prior model: Geophysics, **71**, no. 5, R69–R78, http://dx.doi.org/10.1190/1.2245469.

Mavko, G., T. Mukerji, and J. Dvorkin, 2009, The rock physics handbook: Tools for seismic analysis in porous media: Cambridge University Press.

Schoenberg, M., and C. M. Sayers, 1995, Seismic anisotropy of fractured rock: Geophysics, **60**, 204–211, http://dx.doi.org/10.1190/1.1443748.

Ulvmoen, M., H. Omre, 2010, Improved resolution in Bayesian lithology/fluid inversion from prestack seismic data and well observations: Part1 — Methodology: Geophysics, **75**, no. 2, R21–R35, http://dx.oi.org/10.1190/1.3294570.